Heat and Mass Transfer 39 (2003) 553–560
DOI 10.1007/s00231-002-0354-3

Effects of heat generation on g-Jitter induced natural convection flow in a channel with isothermal or isoflux walls

Ali J. Chamkha

Abstract This paper discusses the behavior of g-jitter induced free convection in microgravity under the influence of a transverse magnetic field and in the presence of heat generation or absorption effects for a simple system consisting of two parallel impermeable infinite plates held at four different thermal boundary conditions. The governing equations for this problem are derived on the basis of the balance laws of mass, linear momentum, and energy modified to include the effects of thermal buoyancy, magnetic field and heat generation or absorption as well as Maxwell's equations. The fluid is assumed to be viscous, Newtonian and have constant properties except the density in the body force of the balance of linear momentum equation. The governing equations are solved analytically for the induced velocity and temperature distributions as well as for the electric field and total current for electrically-conducting and insulating walls. This is done for isothermal–isothermal, isoflux–isothermal, isothermal–isoflux and isoflux–isoflux thermal boundary conditions. Graphical results for the velocity amplitude and distribution are presented and discussed for various parametric physical conditions.

1 Introduction

Natural convection flows in vertical channels have received considerable attention because of their wide-spread application in many geophysical and engineering problems such as cooling of electronic equipment, heating of the Trombe wall system, gas-cooled nuclear reactors, and others. Aung (1972) and Aung and Worku (1986) have studied the thermal and flow characteristics as well as the conditions for flow reversal associated with steady fully-developed flow in a vertical parallel plates channel.

The problem of unsteady laminar developing free convection flow in a vertical channel has been solved numerically by many investigators such as Joshi (1988), Lee et al. (1982), Yang et al. (1974) and Kettleborough (1972). Wang (1988) has solved the problem of unsteady fully-developed free convection in a vertical channel with periodic heat input.

Received: 13 September 1999
Published online: 14 May 2003

A.J. Chamkha
Department of Mechanical Engineering, Kuwait University,
P. O. Box 5969, Safat, 13060 Kuwait
E-mail: chamkha@kuc01.kuniv.edu.kw

Natural convection flow due to temperature gradient and gravity is known to have a profound effect on the homogenous melt growth of semiconductor or metal crystals on earth-bound conditions. In space, the gravity effect is reduced significantly and so is the buoyancy effect due to it. However, while microgravity environment is helpful in reducing convective flows, the effect of g-jitter or residual accelerations which come from crew motions, mechanical vibrations (pumps, motors, excitations of natural frequencies of spacecraft structure), spacecraft maneuvers, atmospheric drag and the earth's gravity gradient (Antar and Nuotio-Antar, 1993 and Li 1996) have shown to make it difficult to realize a diffusion-controlled growth from melts in microgravity (Lehoczky, 1994). This adverse effect of g-jitter has been the subject of many investigations (see, for instance, Jacqmin, 1990, Alexander, 1994, and Chen and Saghir, 1994).

The application of a magnetic field in electrically-conducting fluids such as liquid metals have shown to damp the flow velocities in the liquid. This produces less convective flows. Magnetic damping has been widely used in the semiconductor industries (Series and Hurle, 1991). In many situations, heat generation or absorption may be significant. This effect has a profound influence on the thermal and induced flow characteristics of buoyancy-induced flows (see Vajravelu and Nayfeh, 1992, Chamkha 1997, and Vajravelu and Hadjinicolaou, 1997). Li (1996) has considered g-jitter induced free convection in a transverse magnetic field for a simple system consisting of two parallel plates held at equal or different temperatures. Li (1996) did not consider the possibility of having other thermal or heating conditions at the walls.

In this paper, the behavior of g-jitter induced free convection in microgravity under the influence of a transverse magnetic field is analyzed for a simple system consisting of two parallel impermeable infinite plates (channel) held at four different thermal boundary conditions. Our objective is to develop a basic understanding of the interaction between the applied magnetic field and the oscillating flows associated with the g-jitter for the different wall heating conditions and in the presence of heat generation or absorption effects. Various limiting cases based on the general solution are examined.

2 Governing equations

Consider laminar, fully-developed, free convection flow of a Newtonian, electrically-conducting and heat-generating

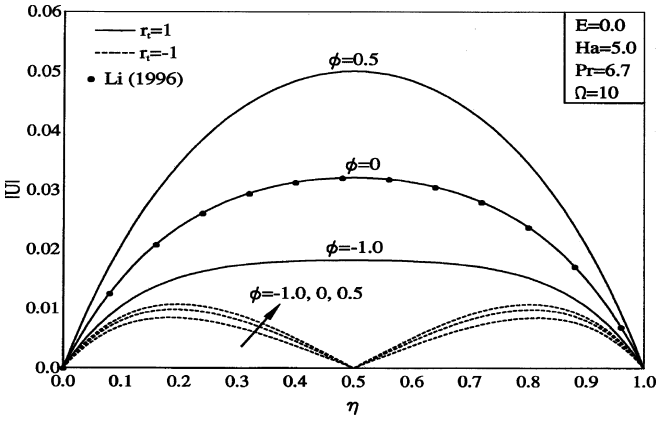

Fig. 1. Effects of ϕ on |U| for isothermal–isothermal walls

or absorbing fluid at a temperature T_o between two infinitely long impermeable parallel plates caused by a temperature gradient or different heating conditions at the plates in the presence of a transverse magnetic field (see Figure 1). The left wall is maintained at a constant temperature T_1 or a constant heat flux q_1 while the right wall is maintained at a constant temperature T_2 or a constant heat flux q_2. The gravity field is assumed to be spatially constant and oscillatory with time. The magnetic Reynolds number is assumed to be small so that the induced magnetic field can be neglected. Also, the channel walls are assumed to be electrically non-conducting. All fluid properties are assumed constant except the density in the buoyancy term of the momentum equation. The governing equations for this investigation are based on the balance laws of mass, linear momentum, and energy along with Maxwell equations for the electromagnetic phenomenon. Under the above mentioned assumptions, these equations reduce to

$$\frac{\partial u}{\partial t} = \nu\frac{\partial^2 u}{\partial y^2} + g(t)\beta_T(T - T_o) - \frac{\sigma}{\rho}(E_z + B_o u)B_o \tag{1}$$

$$\frac{\partial T}{\partial t} + u\frac{\partial T}{\partial x} = \alpha\frac{\partial^2 T}{\partial y^2} + \frac{Q_o}{\rho c_p}(T - T_o) \tag{2}$$

$$\frac{\partial B_x}{\partial t} = -\frac{\partial E_z}{\partial y} \tag{3}$$

where t is time, x and y are the vertical and horizontal distances, respectively. u and T are the fluid vertical velocity component and temperature, respectively. ν, ρ, σ, α, c_p and Q_o are the fluid kinematic viscosity, density, electrical conductivity, thermal diffusivity, specific heat, and the dimensional heat generation or absorption coefficient, respectively. β_T, B_o, B_x, and E_z are the fluid thermal expansion coefficient, the applied magnetic field, the x-component of the magnetic induction, and the electric field component normal to the x-y plane. g(t) is the residual gravity field or g-jitter.

For a time harmonic or oscillatory g-jitter with a frequency ω such as that occurring in space due to mechanical vibrations, $g(t)=g_o e^{j\omega t}$ (g_o being the g-jitter magnitude and j being the complex number index such that $j^2=-1$), the flow field as well as the induced electric field will have a similar oscillatory behavior. That is, $u=u_o e^{j\omega t}$ and $E_z=E_o e^{j\omega t}$ where u_o and E_o are functions of y only.

The physical dimensional boundary conditions for this problem are given by

$$u(t,0) = 0, \quad u(t,L) = 0 \tag{4a, b}$$

$$T(t,0) = T_1 \quad \text{or} \quad q_1 = -k\frac{\partial T}{\partial y}(t,0) \tag{4c, d}$$

$$T(t,L) = T_2 \quad \text{or} \quad q_2 = -k\frac{\partial T}{\partial y}(t,L) \tag{4e, f}$$

where k is the fluid thermal conductivity. Equations (4a,b) indicate no slip conditions at both the left and right walls. Equations (4c,d) correspond to isothermal left wall or isoflux left wall (q_1=constant). Equations (4e,f) correspond to isothermal right wall or isoflux right wall (q_2=constant).

Differentiating Equation (1) with respect to x gives

$$\frac{\partial T}{\partial x} = 0 \tag{5}$$

which means that the fluid temperature is independent of x and, therefore, it will vary with t and y only. Following Li (1996), it is convenient to non-dimensionalize the above equations by using

$$\eta = \frac{y}{L}, \quad \tau = \frac{t\nu}{L^2}, \quad U = \frac{u_o}{u_o^*}, \quad E = \frac{E_o}{E_o^*}, \quad \theta = \frac{(T - T_o)}{\Delta T} \tag{6}$$

where L is the distance between the channel walls, ΔT is the scaling temperature to be defined subsequently, and u_o^* and E_o^* are scaling factors for the velocity and electric field given by

$$u_o^* = \frac{g_o\beta_T(T_2 - T_o)L^2}{\nu}, \quad E_o^* = \frac{g_o\beta_T(T_2 - T_o)L^2B_o}{\nu} \tag{7}$$

Substitution of the oscillatory functions for g(t), u(t, y) and E_z(t, y) and Equations (5) and (6) into Equations (1) through (3) and rearranging yields

$$\frac{d^2U}{d\eta^2} - (j\Omega + Ha^2)U + \theta - Ha^2E = 0 \tag{8}$$

$$\frac{\partial\theta}{\partial\tau} - \frac{1}{Pr}\frac{\partial^2\theta}{\partial\eta^2} - \phi\theta = 0 \tag{9}$$

where

$$\Omega = \frac{\omega L^2}{\nu}, \quad Ha^2 = \frac{\sigma B_o^2 L^2}{\rho\nu}, \quad Pr = \frac{\nu}{\alpha}, \quad \phi = \frac{Q_o L^2}{\nu} \tag{10}$$

are the dimensionless frequency, square of the Hartmann number, Prandtl number, and the dimensionless heat generation or absorption coefficient, respectively.

The dimensionless form of the boundary conditions given by Equations (4a–f) is obtained by using Equations (6) to yield

$$U(\tau,0)=0, \quad U(\tau,1)=0 \tag{11a, b}$$

$$\theta(\tau,0)=r_t, \quad r_{tq} \quad \text{or} \quad \frac{\partial\theta}{\partial\eta}(\tau,0)=-1 \tag{11c, d}$$

$$\theta(\tau,1)=1, \quad r_{qt} \quad \text{or} \quad \frac{\partial\theta}{\partial\eta}(\tau,1)=-1, \quad -r_{qq} \tag{11e, f}$$

where

$$r_t=\frac{T_1-T_o}{T_2-T_o}, \quad r_{tq}=\frac{T_1-T_o}{q_2L/K}, \quad r_{qt}=\frac{T_2-T_o}{q_1L/K}, \quad r_{qq}=\frac{q_2}{q_1} \tag{12}$$

It should be noted here that $\Delta T=T_2-T_o$ for isothermal-isothermal walls, $\Delta T=q_2L/k$ for isothermal-isoflux walls, and $\Delta T=q_1L/k$ for isoflux-isothermal and isoflux-isoflux walls.

3 Analytical solutions

In this section, analytical solutions for the velocity and temperature profiles in the channel are reported for four different thermal boundary conditions. These are the isothermal–isothermal (T_1-T_2), isothermal–isoflux (T_1-q_2), the isoflux–isothermal (q_1-T_2) and the isoflux–isoflux (q_1-q_2) thermal boundary conditions. All of these solutions assume that the temperature field have reached the steady-state conditions.

Without going into detail, it can be shown that the solutions of Equations (9) and (8) for the temperature and velocity distributions in the channel, respectively are given by

$$\theta(\eta)=C_1^*\cosh(s\eta)+C_2^*\sinh(s\eta) \tag{13}$$

$$U(\eta)=C_1\cosh(\beta\eta)+C_2\sinh(\beta\eta)+A\cosh(s\eta)+B\sinh(s\eta)+D \tag{14}$$

where

$$s=i\sqrt{\phi Pr}, \quad \beta=\sqrt{Ha^2+j\Omega} \tag{15}$$

$$A=\frac{-C_1^*}{s^2-\beta^2}, \quad B=\frac{-C_2^*}{s^2-\beta^2}, \quad D=\frac{-Ha^2E}{\beta^2} \tag{16}$$

$$C_1=-A-D,$$
$$C_2=\frac{-A[\cosh(s)-\cosh(\beta)]-B\sinh(s)-D[1-\cosh(\beta)]}{\sinh(\beta)} \tag{17}$$

and

$$C_1^*=r_t, \quad C_2^*=\frac{1-r_t\cosh(s)}{\sinh(s)} \tag{18}$$

for the isothermal–isothermal case,

$$C_1^*=r_{tq}, \quad C_2^*=\frac{-[1+r_{tq}s\sinh(s)]}{s\cosh(s)} \tag{19}$$

for the isothermal–isoflux case,

$$C_1^*=\frac{sr_{qt}+\sinh(s)}{s\cosh(s)}, \quad C_2^*=-\frac{1}{s} \tag{20}$$

for the isoflux–isothermal case, and

$$C_1^*=\frac{\cosh(s)-r_{qq}}{s\sinh(s)}, \quad C_2^*=-\frac{1}{s} \tag{21}$$

for the isoflux–isoflux case.

4 Limiting cases

For the case of asymmetric isothermal wall conditions and in the absence of heat generation or absorption ($\phi=0$), the temperature and velocity profiles in the channel are obtained from Equations (13) and (14) by using the Taylor series expansions of cosh(z) and sinh(z) such that

$$\cosh(z)=1+\frac{z^2}{2}+O(z^4), \quad \sinh(z)=z+\frac{z^3}{6}+O(z^5) \tag{22}$$

(where z is any variable) and letting $\phi\to0$ (or $s\to0$). Doing this, Equation (13) becomes

$$\theta(\eta)=r_t\left(1+\frac{s^2}{2}+\cdots\right)+\frac{\left[1-r_t\left(1+\frac{s^2}{2}+\cdots\right)\right](s\eta+\cdots)}{s+\cdots} \tag{23}$$

Therefore,

$$\lim_{s\to0}\theta(\eta)=r_t+(1-r_t)\eta \tag{24}$$

The velocity distribution can be written as

$$U(\eta)=N_1\cosh(\beta\eta)+N_2\sinh(\beta\eta)+A^*+B^*(s\eta)+D \tag{25}$$

where

$$A^*=\frac{r_t}{\beta^2}, \quad B^*=\frac{1-r_t}{\beta^2 s} \tag{26}$$

$$N_1=\frac{1}{\beta^2}[Ha^2E-r_t],$$
$$N_2=\frac{1}{\beta^2\sinh(\beta)}\left\{(Ha^2E-r_t)[1-\cosh(\beta)]-(1-r_t)\right\} \tag{27}$$

Using the trigonometric identity

$$\sinh(\beta+\beta\eta)=\sinh(\beta)\cosh(\beta\eta)+\cosh(\beta)\sinh(\beta\eta) \tag{28}$$

and rearranging yields

$$U(\eta)=\frac{1}{\beta^2}\left\{\begin{array}{l}(r_t-Ha^2E)+(1-r_t)\eta+\dfrac{(Ha^2E-1)\sinh(\beta\eta)}{\sinh(\beta)}\\ +\dfrac{(Ha^2E-r_t)\sinh[\beta(1+\eta)]}{\sinh\beta}\end{array}\right\} \tag{29}$$

Equations (24) and (29) are exactly the same as those reported earlier by Li (1996).

Furthermore, by using the Taylor series expansion $\sinh(\beta)=\beta+\frac{\beta^3}{6}+O(\beta^5)$, allowing $\beta\to0$ in Equation (14), and neglecting higher-order terms, the following result is obtained

$$\underset{\beta,\phi\to0}{\text{Limit}}\,U(\eta)=(2r_t+1)\frac{\eta}{6}-r_t\frac{\eta^2}{2}+(r_t-1)\frac{\eta^3}{6} \tag{30}$$

Equation (30) gives the same expression obtained by Aung (1972) for fully developed laminar convection between vertical plates heated asymmetrically in the absence of heat generation or absorption and magnetic field effects and where the gravity field is constant.

For the case of a pure g-jitter induced time harmonic motion without the magnetic field, the oscillatory flow velocity in the channel whose amplitude is spatially dependent is obtained by setting Ha=0 in Equation (14) to yield

$$U(\eta)=N_3\cosh\sqrt{j\Omega}\eta+N_4\sinh\sqrt{j\Omega}+A_1\cosh(s\eta)+B_1\sinh(s\eta) \tag{31}$$

where

$$A_1=\frac{-C_1^*}{s^2-j\Omega},\quad B_1=\frac{-C_2^*}{s^2-j\Omega} \tag{32}$$

$$N_3=-A_1,\quad N_4=\frac{-A_1\left[\cosh(s)-\cosh\sqrt{j\Omega}\right]-B_1\sinh(s)}{\sinh\left(\sqrt{j\Omega}\right)} \tag{33}$$

Further, in the limit as $\phi\to0$ (no heat generation or absorption) which means $s\to0$ and with the use of Equations (22) and (28), Equations (31) through (33) combined reduce to

$$\underset{Ha,\phi\to0}{\text{Limit}}\,U(\eta)=\frac{1}{j\Omega}\left\{r_t+(1-r_t)\eta-\frac{\sinh\left(\sqrt{j\Omega}\eta\right)+r_t\sinh\left[\sqrt{j\Omega}(1-\eta)\right]}{\sinh\sqrt{j\Omega}}\right\} \tag{34}$$

which is the same result reported earlier by Li (1996).

For the case of magnetic damping natural convection with heat generation or absorption effects ($\Omega=0$, $\phi\neq0$) under earth-bound conditions, the non-oscillatory velocity profile in the channel reduces to

$$U(\eta)=N_5\cosh(Ha\eta)+N_6\sinh(Ha\eta)+A_2\cosh(s\eta)+B_2\sinh(s\eta)+D_2 \tag{35}$$

where

$$A_2=\frac{-r_t}{s^2-Ha^2},\quad B_2=\frac{r_t\cosh(s)-1}{(s^2-Ha^2)\sinh(s)},\quad D_2=-E \tag{36}$$

$$N_5=-A_2+E,$$

$$N_6=\frac{-A_2[\cosh(s)-\cosh(Ha)]-B_2\sinh(s)+E[1-\cosh(Ha)]}{\sinh(Ha)} \tag{37}$$

Again, as $\phi\to0$, it can be shown that Equation (35) reduces to the solution given by Li (1996) which is

$$U(\eta)=\frac{1}{Ha^2}\left\{\begin{array}{l}(Ha^2E-1)\dfrac{\sinh(Ha\eta)}{\sinh(Ha)}-\\ Ha^2E+r_t+(1-r_t)\eta\\ +(Ha^2E-r_t)\dfrac{\sinh[Ha(1-\eta)]}{\sinh(Ha)}\end{array}\right\} \tag{38}$$

As noted by Li (1996), when $r_t=1$, that is $\theta(\eta)=1$ (uniform temperature in the channel), the above expression reduces to the solution of the classical Hartmann problem with a constant pressure gradient reported by Hughes and Young (1966). For this particular case, the pressure gradient would be normalized to unity. It should be mentioned that similar special cases can be obtained for other cases of isothermal–isoflux, isoflux–isothermal and isoflux–isoflux wall conditions.

5 Total current results

With the velocity distribution in the channel known, the induced current density and the total current can be calculated. The total current is determined by integrating the induced current density $C_d(\eta)=E+U(\eta)$ between the plates. This is given by

$$I=\int_0^1 C_d(\eta)d\eta \tag{39}$$

Substituting the general form of the velocity profile in the channel (Equation (14)) and performing the integration yields

$$I=E+D+\frac{C_1}{\beta}\sinh(\beta)+\frac{C_2}{\beta}[\cosh(\beta)-1]+\frac{A}{s}\sinh(s)+\frac{B}{s}[\cosh(s)-1] \tag{40}$$

In the limit as $s\to0$ ($\phi\to0$), and with the use of Equations (22), (26), and (27), Equation (40) reduces to

$$I=E+\frac{1}{\beta^2}\left\{\frac{r_t+1}{2}-Ha^2E+\frac{[\cosh(\beta)-1]}{\beta\sinh(\beta)}[2Ha^2E-r_t-1]\right\} \tag{41}$$

which is the same expression reported earlier by Li (1996).

Depending on the electric conditions of the vertical plates, the velocity field in the channel can be altered. First, contrary to the working fluid, when the channel walls are electrically non-conducting (insulators), then the total current in the channel flow is zero (I=0). For this situation, the electric field E can be calculated by setting Equation (40) equal to zero and solving for E to give

$$E=\left\{\begin{array}{l}\dfrac{A}{\beta}\sinh(\beta)+\left\{\dfrac{A[\cosh(s)-\cosh(\beta)]+B\sinh(s)}{\beta\sinh(\beta)}\right\}[\cosh(\beta)-1]\\ -\dfrac{A\sinh(s)}{s}+\dfrac{B}{s}[\cosh(s)-1]\end{array}\right\} \Bigg/ \left\{1-\frac{Ha^2}{\beta^2}\left\{1-\frac{\sinh(\beta)}{\beta}+\frac{[1-\cosh(\beta)]^2}{\beta\sinh(\beta)}\right\}\right\} \tag{42}$$

In the limit as s→0, it can be shown that Equation (42) reduces to the expression given by Li (1996) which is

$$E=\frac{1+r_t}{2}\left\{\frac{2\cosh(\beta)-\beta\sinh(\beta)-2}{2Ha^2[\cosh(\beta)-1]+j\Omega\beta\sinh(\beta)}\right\} \tag{43}$$

However, when the channel walls are electrically conducting, the total current in the channel is not zero. But the fact that the tangential electric field must be continuous across the fluid to wall interface requires that the electric field vanishes (see Hughes and Young, 1966 and Li, 1996). In this case, the velocity distribution and the total current in the channel are given, respectively, by

$$U(\eta)=N_7\cosh(\beta\eta)+N_8\sinh(\beta\eta)+A\cosh(s\eta)+B\sinh(s\eta) \tag{44}$$

$$I(\eta)=\frac{N_7}{\beta}\sinh(\beta)+\frac{N_8}{\beta}[\cosh(\beta)-1]+\frac{A}{s}\sinh(s)+\frac{B}{s}[\cosh(s)-1] \tag{45}$$

where

$$N_7=-A,\quad N_8=\frac{-A[\cosh(s)-\cosh(\beta)]-B\sinh(s)}{\sinh(\beta)} \tag{46}$$

In the absence of heat generation or absorption (ϕ=0), Equation (44) can be shown to reduce to the result given by Li (1996) which is

$$U(\eta)=\frac{1}{\beta^2}\left\{r_t+(1-r_t)\eta-\frac{\sinh(\beta\eta)+r_t\sinh[\beta(1-\eta)]}{\sinh(\beta)}\right\} \tag{47}$$

6 Graphical results and discussion

Numerical evaluations of the analytical solutions reported in the previous section are performed and some representative results are illustrated graphically in Figures 1 through 11. These results are selected to show the effects of heat generation or absorption and the various heating conditions at the walls.

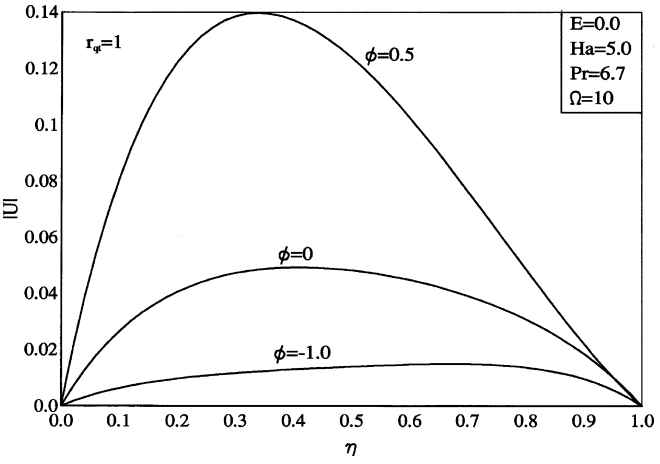

Fig. 2. Effects of ϕ on |U| for isoflux–isothermal walls (r_{qt}=1)

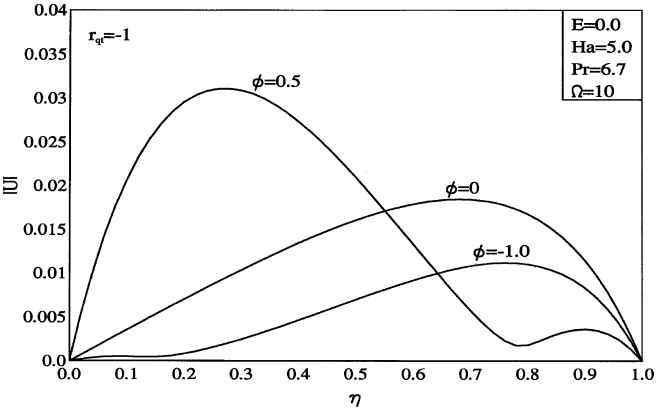

Fig. 3. Effects of ϕ on |U| for isoflux–isothermal walls (r_{qt}=–1)

Figure 1 depicts the influence of the heat generation or absorption ϕ on the flow velocity amplitude |U| for the case of electrically-conducting (E=0) symmetric and asymmetric wall temperature condition for two different temperature gradient situations r_t=1 and r_t=–1. Physically speaking, heat generation causes the temperature distribution in the channel to increase. This causes higher buoyancy-induced flow in the vertical direction. This is reflected in the increases in the velocity amplitude |U| as ϕ increases shown in Figure 1. On the contrary, heat absorption causes decreases in the fluid temperature which produce retardation in the convective flow. It is apparent from Figure 1 that the velocity amplitude |U| for r_t=1 is symmetric in this channel while it approaches a half wave shape for r_t=–1. The results for ϕ=0 are in excellent agreement with those reported by Li (1996).

Figures 2 and 3 illustrate the effect of ϕ on the velocity amplitude |U| for a channel having electrically-conducting (E=0) isoflux–isothermal wall conditions for two different thermal gradient situations r_{qt}=1 and r_{qt}=–1, respectively. As mentioned before, increases in ϕ produce higher induced flow rates in the channel. It is observed from these figures that for ϕ=0.5 while the velocity amplitude remains

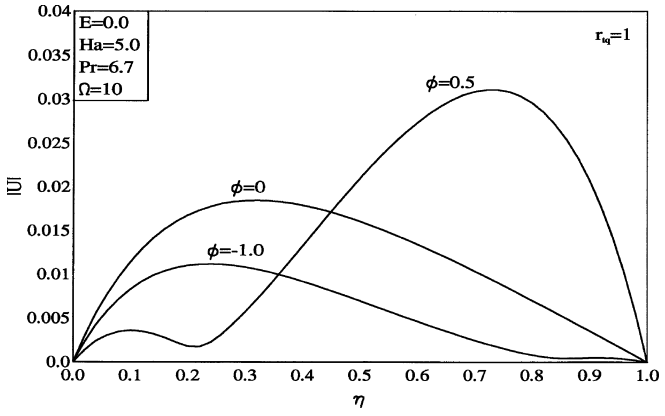

Fig. 4. Effects of ϕ on |U| for isothermal–isoflux walls (r_{tq}=1)

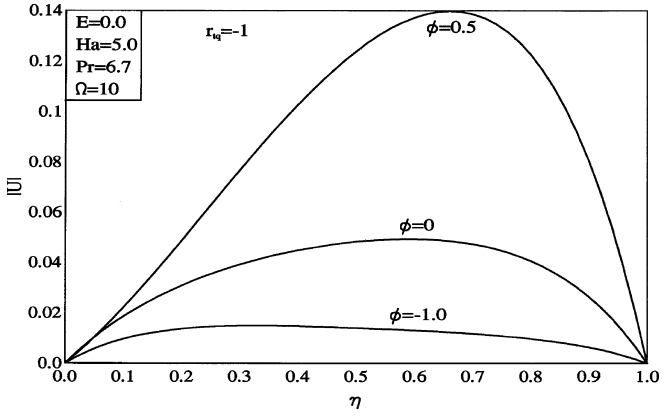

Fig. 5. Effects of ϕ on |U| for isothermal–isoflux walls (r_{tq}=−1)

almost symmetric in the channel for r_{qt}=1, it becomes totally asymmetric for r_{qt}=−1 in which most of the flow occurs close to the isoflux wall with the existence of a small wave-like near the isothermal wall. It is expected that for r_{qt}=1 the profile of |U| becomes more asymmetric and its peak value moves towards the isoflux wall as ϕ is increased beyond 0.5.

Figures 4 and 5 present |U| for various values of ϕ for the case of electrically-conducting isothermal–isoflux wall conditions for the thermal gradients r_{tq}=1 and r_{tq}=−1, respectively. Comparing these figures with Figures 2 and 3, it can be seen that the corresponding opposite effect is produced by reversing the wall thermal conditions in which most of the flow is induced very close to the right isoflux wall for the heat generation case in which ϕ=0.5 and r_{tq}=1 while the flow is almost symmetric in the channel for r_{tq}=−1. It should be noted that for r_{tq}=1 with ϕ=0 or ϕ=−1 the flow close to the isothermal wall is more significant than that near the isoflux wall.

The magnetic damping of the flow velocity amplitude |U| in the channel with electrically-conducting isoflux–isothermal wall conditions is shown in Figure 6. Imposition of a transverse magnetic field normal to the flow direction gives rise to a resistive force called the Lorentz force which causes suppression in the velocity amplitude |U| resulting from increasing the Hartmann number Ha as shown in Figure 6.

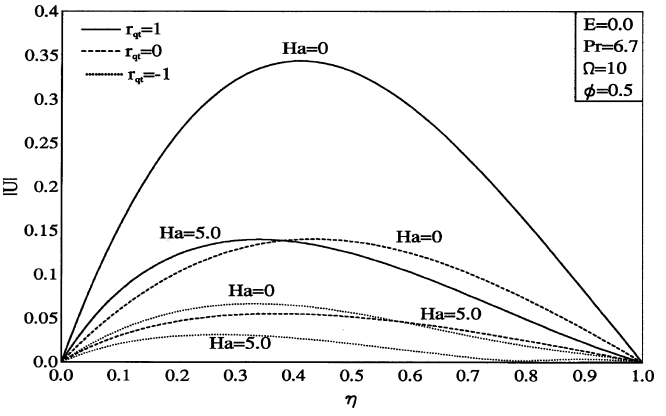

Fig. 6. Effects of Ha on |U| for isoflux–isothermal walls

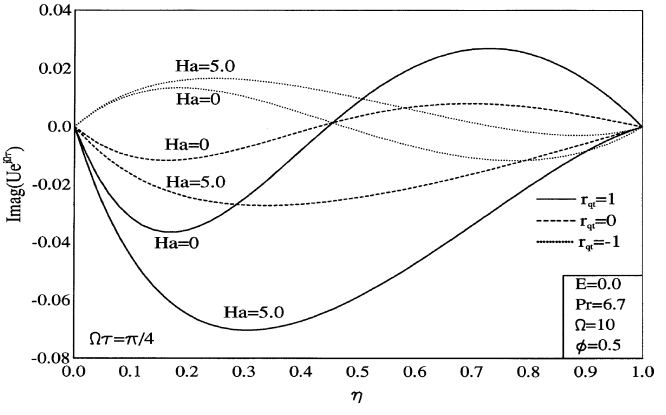

Fig. 7. Effects of Ha on Imag($Ue^{j\Omega\tau}$) for isoflux–isothermal walls

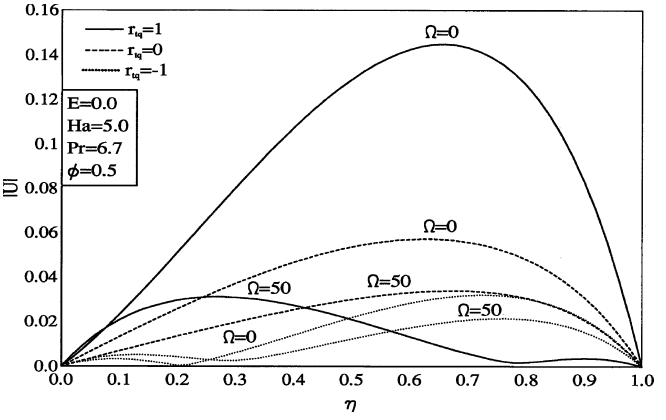

Fig. 8. Effects of Ω on |U| for isothermal–isoflux walls

In Figure 7, the Imag($Ue^{j\Omega\tau}$)=Real(U) sin($\Omega\tau$) + Imag(U) cos($\Omega\tau$), which represents the measurable value of the driving gravity force Imag($g_o e^{j\Omega\tau}$)=g_o sin($\Omega\tau$), within the channel walls is presented for three thermal gradient cases (r_{qt}=−1, 0, 1) of the isoflux–isothermal wall conditions. It is seen that increasing the Hartmann number Ha to 5 diminishes the existence of the wave appearing for Ha=0 for both r_{qt}=0 and r_{qt}=1. However, the oscillatory behavior remains slightly for r_{qt}=−1.

Figure 8 shows the effects of the g-jitter frequency Ω on the flow behavior in the channel for three thermal gradient

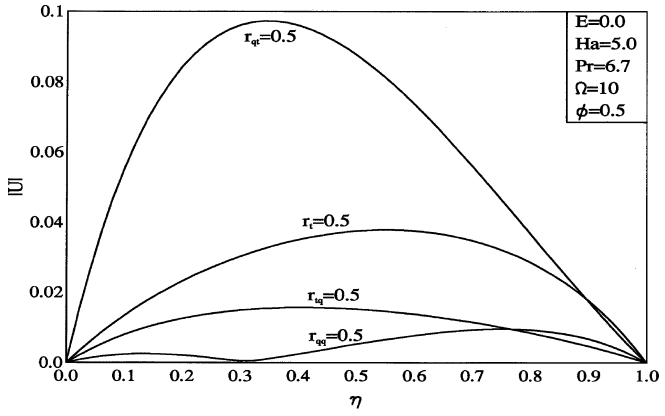

Fig. 9. Effects of thermal gradient parameter on |U|

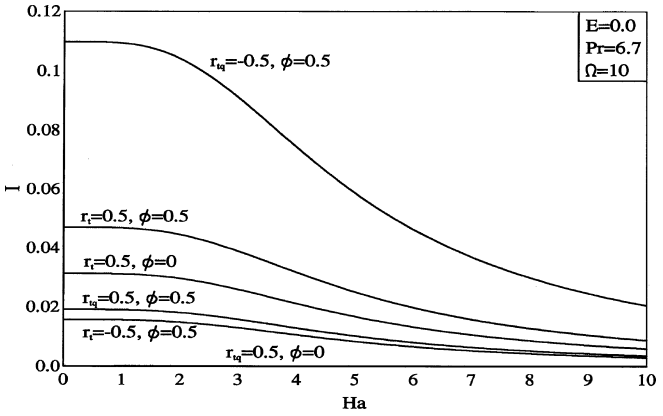

Fig. 11. Effects of Ha, r_t, r_{tq} and ϕ on total current

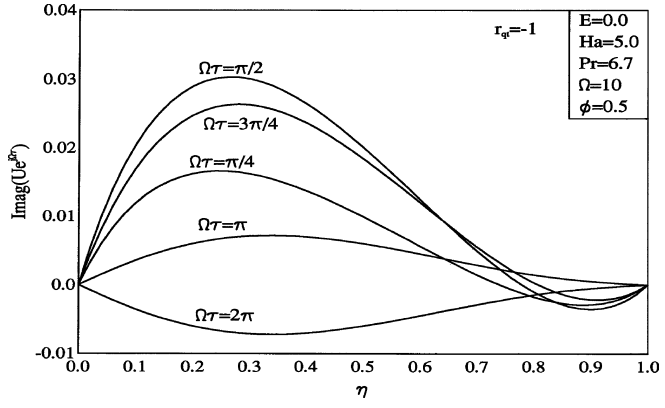

Fig. 10. Effects of $\Omega\tau$ on Imag($Ue^{j\Omega\tau}$) for isoflux–isothermal walls

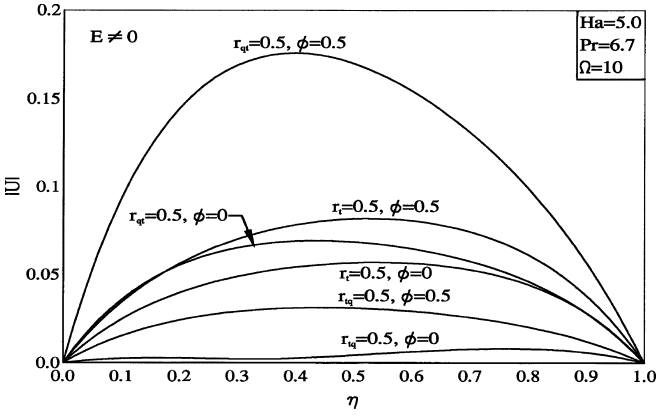

Fig. 12. Flow fields for electrically-insulating walls

cases (r_{tq}=–1, 0, 1) of the electrically-conducting (E=0) isothermal–isoflux wall conditions. Consistent with previous studies, it is predicted that less induced flow in the channel occurs as the g-jitter frequency Ω increases. This suggests that a g-jitter with higher frequency would have less harmful effects in inducing flow variations across the channel.

Figure 9 illustrates the influence of the various thermal gradients for the cases of isothermal–isothermal, isoflux–isothermal, isothermal–isoflux, and isoflux–isoflux wall conditions at the same parametric conditions on the flow velocity in the channel. It is observed that the highest induced flow occurs for the case of isoflux–isothermal walls while the slowest induced flow takes place for the isoflux–isoflux walls. Also, it is noted that a region of zero flow occurs within the channel (η=0.3) for the case where r_{qq}=0.5 and that most of the flow takes place in the regions close to the walls especially the right wall.

Figure 10 depicts the behavior of the flow distribution in the channel for various $\Omega\tau$ values for the electrically-conducting isoflux–isothermal walls with r_{qt}=–1. As obvious from this figure, a small oscillatory behavior of the flow in the channel is predicted. This is in contrast with the well-defined wave oscillation along the η direction with a zero velocity time-invarying nodal point at η=0.5 predicted by Li (1996) for the case of isothermal–isothermal walls with r_t=–1 and in the absence of heat generation (ϕ=0).

Figure 11 shows the effects of Ha, ϕ and the thermal gradient coefficients r_t and r_{tq} on the total current I for electrically-conducting channel walls. It is predicted that the total current in the channel decreases with increases in the values of Ha. In addition, the effect of heat generation (ϕ>0) is found to increase the total current in the channel for all values of Ha. Also, as the thermal gradient coefficient for isothermal–isothermal walls (r_t) increases, the total current I is observed to increase. However, the opposite occurs when the thermal gradient coefficient for isothermal–isoflux walls (r_{tq}) increases.

Figure 12 displays the effects of ϕ on the velocity amplitude |U| for electrically-insulating (E ≠ 0) isothermal–isothermal and isothermal–isoflux channel walls. For this situation the electric field E is calculated from Equation (42). Comparison of this figure with Figure 9 shows that the magnetic damping effect through the application of the magnetic field is much stronger for the case of electrically-conducting channel walls than for electrically-insulating walls. This is consistent with the conclusion of Li (1996).

7 Conclusion

The problem of g-jitter or residual acceleration induced free convection flow of an electrically-conducting and heat generating or absorbing fluid through a parallel-plate

channel in the presence of a transverse uniform magnetic field was considered. The walls of the channel were held at constant temperature or heat flux and were either electrically-conducting or electrically-insulating. Four different combinations of wall thermal conditions were considered. These were the isothermal–isothermal, isoflux–isothermal, isothermal–isoflux and the isoflux–isoflux conditions. The governing equations for this investigation were derived and solved in closed form for the velocity and temperature distributions in the channel. In addition, based on the wall electric conditions, analytical expressions for the total current and the induced current in the channel were derived. Various limiting cases were reported and favorable comparisons with previously published work were obtained. It was found that enhanced induced convective flows in the channel were obtained when the fluid heat generation effect was considered. The opposite behavior was predicted when the fluid heat absorption effect was included. In addition, higher induced flow rates and a less oscillatory flow behavior in the channel were predicted for isoflux–isothermal walls than for isothermal–isothermal walls. On the contrary, lower flow rates were predicted for the isoflux–isoflux walls than for the isothermal–isothermal walls. Also, for the case of isoflux–isoflux walls, most of the flow took place close to the walls with zero flow in the middle of the channel. Moreover, the magnetic damping effect on the flow is much stronger for the cases of electrically-conducting walls than for electrically-insulating walls. It is hoped that the various induced flow behaviors for the different wall conditions predicted in this work in addition to the effect of heat generation or absorption will serve as vehicle for selecting a well-behaved flow condition for semi-conductor crystal growth under terrestrial conditions.

References

Alexander, J. I. D., Residual gravity effects on fluid processes, Microgravity Sci. Technol. 2, 131, 1994

Antar, B. N., and Nuotio-Antar, V. S., Fundamentals of Low Gravity Fluid Dynamics and Heat Transfer. CRC press, Boca Raton, FL, 1993

Aung, W, Fully developed laminar convection between vertical plates heated asymetrically, Int. J. Heat Mass Transfer 15, 577–580, 1972

Aung, W. and Worku, G., Theory of fully developed, combined convection including flow reversal, J. Heat Transfer 108, 485, 1986

Chamkha, A. J., Non-Darcy fully developed mixed convection in a porous medium channel with heat generation/absorption and hydromagnetic effects, Numerical Heat Transfer 32, 653–675, 1997

Chen, H., Saghir, M. Z., Quon, D. H. H., and Chehab, S., Numerical study on transient convection in float zone induced by g-jitter, J. Crystal Growth 142, 362, 1994

Hughes, W. F., and Young F. J., The Electromagnetohydrodynamics of Fluids, John Willey and Sons, New York, 1966

Jacqmin, D., Stability of an oscillating fluid with a uniform density gradient, J. Fluid Mech. 219, 449, 1990

Joshi, H. M., Transient effects in natural convection cooling of vertical parallel plates, Int. Commun. Heat Mass Transfer 15, 227–238, 1988

Kettleborough, C. F., Transient laminar free convection between heated vertical plates including entrance effects, Int. J. Heat Mass Transfer 15, 883–896, 1972

Lee, T. S., Parikh, P. G., Acrivos, A., and Bershader, D., Natural convection in a vertical channel with opposing buoyancy forces, Int. J. Heat Mass Transfer 25, 499–511, 1982

Lehoczky, S., Szofran, F. R., and Gillies, D. C., Growth of solid solution single crystals. Second United States Microgravity Payload, Six Month Sciences Report, NASA MSC, 1994

Li, B. Q., g-Jitter induced free convection in a transverse magnetic field, Int. J. Heat Mass Transfer 39, 2853–2860, 1996

Schneider, S., and Straub, J., Influence of Prandtl number on laminar natural convection in a cylinder caused by g-jitter, J. Crystal Growth 97, 235, 1989

Series, R. W., and Hurle, D. T. J., The use of magnetic fields in semiconductor crystal growth, J. Crystal Growth 113, 305, 1991

Vajravelu, K. and Hadjinicolaou, A., Convective heat transfer in an electrically conducting fluid at a stretching surface with uniform free stream, Int. J. Eng. Sci. 35, 1237–1244, 1997

Vajravelu, K. and Nayfeh, J., Hydromagnetic convection at a cone and a wedge, Int. Commun. Heat Mass Transfer 19, 701–710, 1992

Wang, C. Y., Free convection between vertical plates with periodic heat input, J. Heat Transfer 110, 508–511, 1988

Yang, J. W., Scaccia, C., and Goodman, J., Laminar natural convection about vertical plates with oscillatory surface temperature, ASME J. Heat Transfer 96, 9–14, 1974